Electronic structure of Nb-Mo alloys

E. Colavita, A. Franciosi, R. Rosei, and F. Sacchetti
Istituto di Fisica dell'Università di Roma e Gruppo Nazionale di Struttura della Materia del CNR, Rome, Italy

E. S. Giuliano and R. Ruggeri
Istituto di Fisica dell'Università di Messina, Messina, Italy

D. W. Lynch
Ames Laboratory-USDOE and Department of Physics, Iowa State University, Ames, Iowa 50011
(Received 14 May 1979)

Thermoreflectance measurements on Nb_xMo_{1-x} alloys ($x = 0.2$, 0.5, 0.8) have been carried out in the 0.5–5.0 eV energy region. Augmented-plane-wave (APW) calculations for Nb at two different lattice parameters and for Mo, as well as coherent-potential-approximation calculations (CPA), have been carried out and have been used in the interpretation of the experimental results. Several optical transitions [$\Sigma_1(E_F)\rightarrow\Sigma_3$, $G_4(E_F)\rightarrow G_1$, $N_2\rightarrow N'_1$], have been identified, and their concentration dependence followed. These results contribute significantly toward putting the interpretation of the optical properties of Nb, Mo, and their alloys on a much more secure footing. In particular, it has been confirmed that while the lower conduction bands behave roughly as predicted by the rigid-band model, the higher-lying conduction bands show distinctly non-rigid-band-like behavior.

I. INTRODUCTION

The study of the optical properties of alloys can yield an improved understanding of the optical properties and electronic structure of the pure host metal as well as a better understanding of the alloy system.[1-3] Optical measurements probe the electronic structure at energies several electron volts above and below the Fermi energy, a region untouched by sophisticated "Fermi-surface" measurements. Moreover, the latter measurements rarely can be carried out on alloys. In the following, we report thermoreflectance measurements on Nb-Mo alloys, the optical spectra of which already have been published.[4] These data do indeed provide a better understanding of the optical properties of pure Nb and Mo, and several previously discussed assignments of transitons are confirmed or altered.

Nb and Mo have nearly the same electronic band structure, especially at and below the Fermi level. The Fermi level is higher in Mo than in Nb because of the extra valence electron per atom, and the lattice parameters differ. In such a situation the rigid-band model is expected to be valid.[5] The optical spectra of Nb-Mo alloys would then be interpreted on the basis of a Fermi level which rises as Mo is added to Nb, creating new initial states for optical transitions and destroying final states. However, recent coherent-potential-approximation (CPA) calculations on the Nb-Mo system[6] have shown that the rigid-band model is a poor one for much of the energy range above the Fermi level. They also indicate remarkably little increase in scattering upon alloying in this system. These calculations are described further below. The lack of increased broadening in the alloys is evident in the measured spectra, and the predicted non-rigid-band behavior is found to be necessary to explain the shift upon alloying of the energy of one of the spectral features. The CPA calculations yield a decomposition of states into different angular momentum components, and this is used to explain shifts in strength of several structures as the Nb : Mo ratio changes. An augmented-plane-wave (APW) calculation has been carried out for Nb at two values of the lattice parameter, from which deformation potentials at critical points have been estimated. These reinforce the assignment of one critical-point transition in the thermomodulation spectra, for it is a transition expected to be particularly volume sensitive.

The principal structures which have been identified and followed across the composition range are a transition at 1.62 eV in Nb from the Fermi surface [$\Sigma_1(E_F)\rightarrow\Sigma_3$], which changes to a transition to the Fermi surface [$\Sigma_1\rightarrow\Sigma_3(E_F)$] in $Nb_{0.5}Mo_{0.5}$, a Fermi-surface transition between parallel bands along Σ occurring at 2.26 eV in the entire composition range, and an M_3 critical-point transition ($N_2\rightarrow N'_1$) at 4.53 eV in Nb and near this energy in Mo.

II. EXPERIMENTAL

The thermoreflectance spectra $\Delta R/R$ were measured with a Hilger and Watts quartz prism mono-

chromator and a Hamamatsu R 453 photomultiplier. In the 0.5–1.5 eV energy range a PbS detector was used. The samples were small platelets (about $2\times3\times0.1$ mm^3 in size) cut with a diamond saw from the same electron-beam-melted ingots used in Ref. 4, and prepared in the same way: they were lapped and polished to a mirror finish, then electro-polished (6 vol % sulfuric acid in methanol at dry-ice temperature). They were then glued on a Cr film evaporated on a sapphire substrate, which was, in turn, firmly attached to the cryostat cold finger. The Cr film was used as a heater by passing a 2-Hz unipolar square wave through it with average power up to 10 W. Particular care was taken to ensure an extremely thin layer of glue between sample and heater. This minimizes tiny movements of the sample in phase with the temperature wave which may cause a spurious background signal. Selection of a region of the photocathode which had a homogeneous response also minimized this background signal. The temperature variation at the sample surface (a few degrees Kelvin) causes the modulation in reflectance which was detected by a lock-in amplifier. Signals of several parts in 10^4 were always detected, even for the most concentrated alloy. The accuracy depends somewhat on sample composition and is worse at the extrema of the measured spectra, but is always better than ~3%.

The results are shown in Figs. 1 and 2, together with the spectra for the pure metals Nb and Mo taken from a recent study on transition metals.[7] In this way the evolution of the spectra on going from the pure metals toward the 50% alloy can be followed more easily.

As already pointed out,[7] the Nb spectrum agrees quite well in overall shape with the thermoreflectance results obtained on an opaque Nb film.[8] The spectra obtained from Nb bulk samples, however,

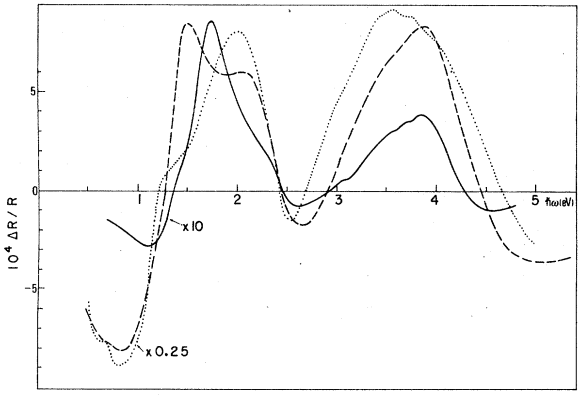

FIG. 1. Thermoreflectance spectra of Nb-Mo alloys. Full line: Nb. Dashed line: $Nb_{0.80}Mo_{0.20}$. Dotted line: $Nb_{0.50}Mo_{0.50}$.

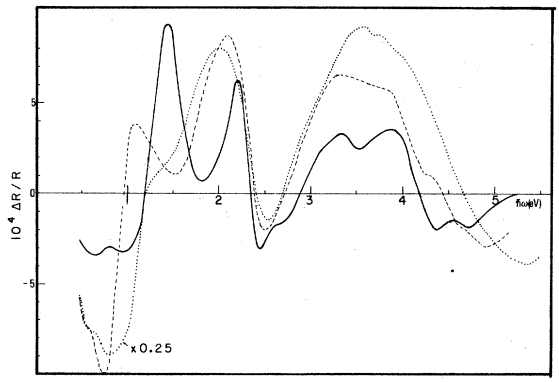

FIG. 2. Thermoreflectance spectra of Nb-Mo alloys. Full line: Mo. Dashed line: $Nb_{0.20}Mo_{0.80}$. Dotted line: $Nb_{0.50}Mo_{0.50}$.

contain further information in the form of fine details (shoulders at 1.38 and 2.36 eV and very tiny structures at 3.05, 3.55, and 3.73 eV). The results for Mo also agree very well with those obtained by Dallaporta *et al.*[9] who, however, present their data with the phase inverted. This agreement confirms that the shoulder detected in Ref. 10 at 1.3 eV and interpreted as arising from spin-orbit $\Delta_5 \rightarrow \Delta_2'$ transitions should be considered as an artifact of the film measurements (probably arising from strains in the film).

Nb presents a very strong feature (positive peak) at 1.74 eV which, upon alloying with Mo, drifts toward lower energies (positive peak at 1.50 eV in $Nb_{0.80}Mo_{0.20}$) and then tends to disappear while continuing to shift (shoulder at 1.30 eV for $Nb_{0.50}Mo_{0.50}$). Upon alloying with molybdenum the negative feature at 1.1 eV also shifts toward lower energies and becomes structured (double-negative peak at 0.5 and 0.8 eV). The shoulder at 2.3 eV in Nb quickly becomes a dominant feature in the 80/20 alloy without appreciably changing its energy. The next structure, consisting of a broad positive peak followed by a broad negative peak, becomes more prominent, relative to the structure at ~2 eV, upon alloying with molybdenum.

Even the more concentrated alloy (50/50) shows traces of some fine structure, but it is difficult to correlate them with the shoulders which Nb shows at 3.05, 3.55, and 3.73 eV.

The first structure in molybdenum has the same general shape found for Nb and other transition metals of the VB and VIB group, but the negative lobe is more structured. Upon alloying with Nb the first positive peak initially shifts toward lower energies, then moves back again. At 2.35 eV we find the zero crossing of a typical derivative feature. This structure stays approximately in the same position upon alloying with Nb, but broadens

noticeably. At higher energies we find again a broad positive peak and a broad negative lobe. Both are structured in Mo but this structure becomes progressively lost on alloying, while the zero crossing moves to higher energies.

As is the case for most transition metals,[7-11] the thermoreflectance spectra of Nb and Mo tend to be rather broad, making the interpretation a challenging problem. One may expect that the spectra of their alloys, especially when concentrated, would tend to be prohibitively broadened, making any attempt to interpret (or even measure) them hopeless.[3] This is shown not to be the case, and even the $Nb_{0.50}Mo_{0.50}$ sample gave a fairly strong signal not excessively broadened, as predicted by recent theoretical work.[6] The broadening is a result of the large phase space into which excitations can scatter. The lack of increased scattering upon alloying and the lack of temperature-dependent broadening in the thermomodulation line shapes indicate that the scattering is largely electron-electron scattering.

III. SPECTRAL FUNCTION AND BAND STRUCTURE

In a perfect crystal the interpretation of the structures found in the measurements is usually supported by some band-structure calculation, and the relevant peaks are connected on physical grounds with transitions between appropriate crystal states. In a random alloy no band structure exists in the conventional sense, and one is faced with a much more difficult problem.[12] However, it has been shown recently[6,13] that, even in such systems, it is possible to compute a function, the so-called Bloch spectral function, $\bar{A}_B(\vec{k},E)$, which is strictly connected with the individual "bands" in the alloy.[14]

To define $\bar{A}_B(\vec{k},E)$, we recall that within the Korringa-Kohn-Rostoker (KKR)-CPA framework[15] the alloy-averaged density of states $\bar{n}(\epsilon)$ can be computed in terms of the matrix elements $\mathcal{J}^c_{LL'}$ of Gyorffy's coherent-scattering-path operator.[16] Such matrix elements are obtained by solving self-consistently the equations

$$\mathcal{J}^c_{LL'}(\epsilon)=\frac{1}{\Omega_{Bz}}\int_{Bz} d^3k\, \mathcal{J}^c_{LL'}(\vec{k},\epsilon)$$

$$=\frac{1}{\Omega_{Bz}}\int_{Bz} d^3k[t_c^{-1}(\epsilon)-G^0(\vec{k},\epsilon)]^{-1}_{LL'}, \quad (1)$$

$$t^{-1}_{c,L}(\epsilon)=\langle t_L^{-1}\rangle+[t^{-1}_{c,L}(\epsilon)-t^{-1}_{A,L}(\epsilon)]\mathcal{J}^c_{LL}(\epsilon)\times[t^{-1}_{c,L}(\epsilon)-t^{-1}_{B,L}(\epsilon)], \quad (2)$$

where L indicates both l and m quantum numbers, $t_{(A,B),L}(\epsilon)$ are given by

$$t_{(A,B),L}(\epsilon)=-\frac{1}{\sqrt{\epsilon}}\sin\delta_L^{A,B}(\epsilon)\exp[i\delta_l^{A,B}(\epsilon)], \quad (3)$$

in which $\delta_l^{A,B}(\epsilon)$ are the phase shifts for the atoms A and B, respectively, and

$$\langle t_L^{-1}\rangle=ct^{-1}_{A,L}(\epsilon)+(1-c)t^{-1}_{B,L}(\epsilon). \quad (4)$$

The $G^0(\vec{k},\epsilon)$ are the well-known structure constants entering the KKR band-structure method.[15]

When Eqs. (1) and (2) have been solved, one can compute the density of states $\bar{n}(\epsilon)$ as the energy derivative of

$$N(\epsilon)=N^0(\epsilon)-\frac{1}{\pi\Omega_{Bz}}\mathrm{Im}\int_{\Omega_{Bz}} d^3k\ln\det[t^{-1}_{c,L}(\epsilon)\delta_{LL'}-G^0_{LL'}(\vec{k},\epsilon)]$$
$$+\frac{c}{\pi}\mathrm{Im}\sum_L\left(\frac{t^{-1}_{B,L}(\epsilon)-\langle t_L^{-1}\rangle}{t^{-1}_{B,L}(\epsilon)-t^{-1}_{c,L}(\epsilon)}\right)+\frac{(1-c)}{\pi}\mathrm{Im}\sum_L\left(\frac{t^{-1}_{A,L}(\epsilon)-\langle t_L^{-1}\rangle}{t^{-1}_{A,L}(\epsilon)-t^{-1}_{c,L}(\epsilon)}\right), \quad (5)$$

where $N^0(\epsilon)$ is the free-electron integrated density of states. Now for a perfect crystal we can define the Bloch spectral function

$$A_B(\vec{k},\epsilon)=\sum_n\delta(\epsilon-\epsilon_n), \quad (6)$$

where n is the band index. We also have

$$n(\epsilon)=\frac{1}{\Omega_{Bz}}\int_{Bz} d^3k A_B(\vec{k},\epsilon), \quad (7)$$

so that $A_B(\vec{k},\epsilon)$ is the density of states per $\vec{k}$ point in the Brillouin zone. To find an analog of Eq. (6) in disordered alloys, we can write Eq. (5) as a single sum over the Brillouin zone, then differentiate with respect to ϵ. After some straightforward algebra we get

$$\bar{A}_B(\vec{k},\epsilon)=A^0_B(\vec{k},\epsilon)+\frac{1}{\pi}\mathrm{Im}\sum_L\left[\frac{\partial}{\partial\epsilon}G^0_{LL}(\vec{k},\epsilon)-[t^{-1}_{A,L}(\epsilon)-t^{-1}_{B,L}(\epsilon)]^{-1}\times\left([t^{-1}_{A,L}(\epsilon)-t^{-1}_{c,L}(\epsilon)]\frac{\partial}{\partial\epsilon}t^{-1}_{B,L}(\epsilon)-[t^{-1}_{B,L}(\epsilon)-t^{-1}_{c,L}(\epsilon)]\frac{\partial}{\partial\epsilon}t^{-1}_{A,L}(\epsilon)\right)\right]\mathcal{J}^c_{LL}(\vec{k},\epsilon), \quad (8)$$

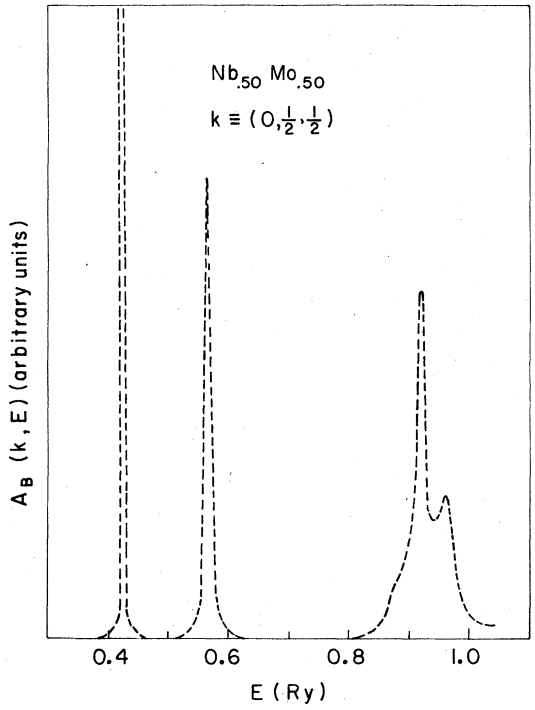

FIG. 3. Bloch spectral function for $Nb_{0.50}Mo_{0.50}$ at the N point of the Brillouin zone.

where $A_B^0(\vec{k}, \epsilon)$ is the free-electron contribution. By definition

$$\bar{n}(\epsilon) = \frac{1}{\Omega_{Bz}} \int_{Bz} d^3k \bar{A}_B(\vec{k}, \epsilon) , \tag{9}$$

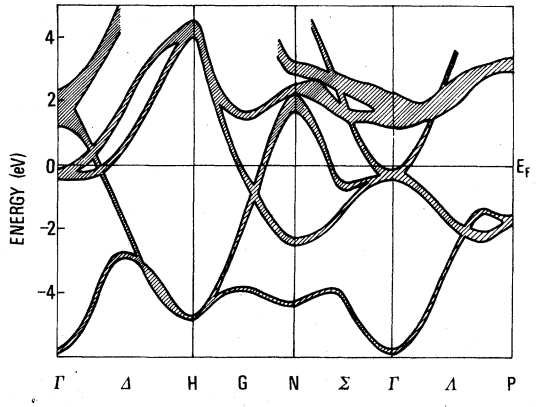

FIG. 4. Pseudoband structure for $Nb_{0.50}Mo_{0.50}$ alloy.

and $\bar{A}_B(\vec{k}, \epsilon)$ can be integrated as the probability that an electron with wave vector $\vec{k}$ has energy ϵ. Clearly $\bar{A}_B(\vec{k}, \epsilon)$ is as close as we can get to looking at individual bands in a random alloy.

In Fig. 3 we show the spectral function for the $Nb_{0.05}Mo_{0.50}$ alloy at the N point as an example. As is shown in the theory, the broadening depends mainly on energy, so that the behavior in other regions can be inferred easily.

The results for the spectral functions can be combined in a pseudoband structure, where each energy level is given by the center of mass of an individual peak of the spectral function and the width of the dispersion curve is given by its full width at the half maximum. In Fig. 4 we show the pseudoband structure for the $Nb_{0.50}M_{0.50}$ alloy.

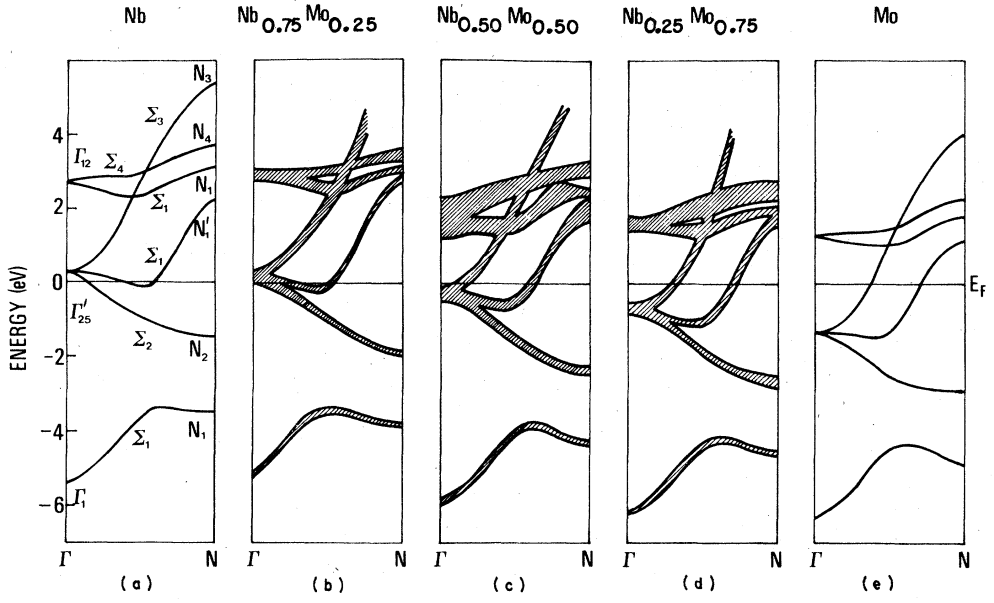

FIG. 5. Band structure of Nb, Mo, and their alloys along the Γ-N direction.

TABLE I. Principal energy levels (eV) for niobium at two different lattice parameters.

	Γ_1	Γ'_{25}	Γ_{12}	H_{12}	H'_{25}	N_{1l}	N_2	N'_1	N_{1u}	N_4	N'_3
$a=a_0$ [a]	3.81	9.50	11.82	5.51	14.33	5.69	7.75	11.40	12.31	12.76	14.60
$a=0.97a_0$	4.29	9.68	12.20	5.29	15.48	5.68	7.80	12.31	12.80	13.34	15.40
E	+0.48	+0.18	+0.38	−0.22	+1.15	−0.01	+0.05	+0.91	+0.49	+0.58	+0.80

[a]Room-temperature value $a_0=6.327$ a.u. (Ref. 22).

The broadening of the bands is fairly small, of the order of 0.2–0.4 eV over most of the energy region shown. The overall behavior of the bonding part of the d-band complex is rigid-band-like, as expected. However, the antibonding part deviates considerably from this simple picture, as discussed in detail in Ref. 3.

In order to follow the behavior of the alloy system up to the extrema of concentration (pure Nb and pure Mo), we have calculated the band structure of the pure metals with an APW formalism[17] *using the same potential* as in the KKR-CPA calculation. We report in Fig. 5 the results of our calculations for the Γ-N direction for the entire range of concentrations.

The APW method has been used for calculating the energy bands for niobium also at a reduced lattice parameter ($a=0.97a_0$). This allows us to determine the deformation potentials for the principal energy levels, which is useful as a guide to specific gaps or regions of the Brillouin zone. The results of these calculations are summarized in Table I.

IV. DISCUSSION

The most efficient way to try to interpret modulated optical spectra is by studying the modulated dielectric-function, $\Delta\tilde{\epsilon}$, spectra.[18] This is especially so for transition metals and their alloys, where optical structures tend to be smeared by matrix-element effects and lifetime broadening. The variation of the imaginary part of the dielectric constant $\Delta\epsilon_2$ is directly correlated to the change in absorption induced by the modulated parameter (in our case the temperature). Furthermore, correlation of structures in $\Delta\epsilon_1$ and $\Delta\epsilon_2$ gives further insight on the origin of optical transitions in k space.

We have determined accordingly $\Delta\epsilon_1$ and $\Delta\epsilon_2$ spectra for all the alloys through Kramers-Kronig analysis of $\Delta R/R$. The static optical constants needed in the inversion were taken from Ref. 4. The results are shown in Fig. 6. The spectra of Nb and Mo, taken from Ref. 7, are also shown for completeness. It is convenient to analyze the results by dividing them into two series, each starting from one of the pure metals. For convenience we report in Fig. 7 the $\Delta\epsilon_2$ spectra of the first series (Nb, $Nb_{0.80}Mo_{0.20}$, $Nb_{0.50}Mo_{0.50}$) superimposed, so that the trends in behavior of the structures upon alloying become more apparent.

As already noted,[7] it often is difficult to recognize specific critical points or Fermi-surface structures[19] in the optical spectra of transition metals, since they can be distorted by matrix-

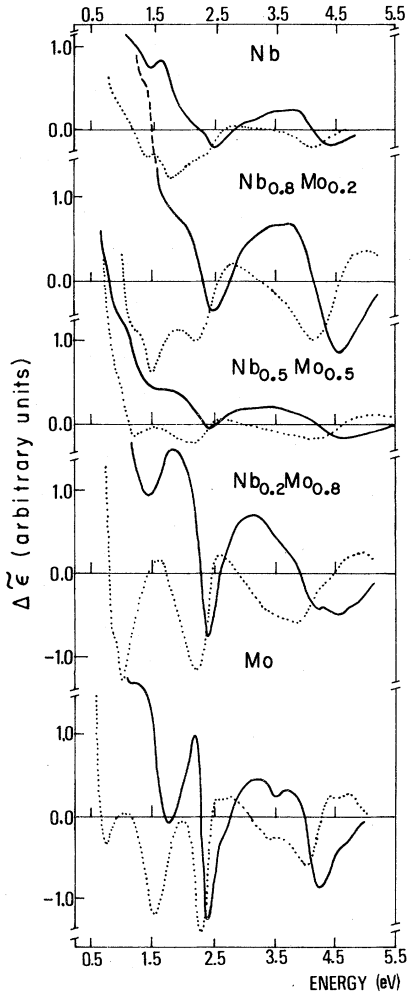

FIG. 6. $\Delta\tilde{\epsilon}$ thermomodulation spectra for Nb, Mo, and their alloys. Full line: $\Delta\epsilon_2$. Dotted line: $\Delta\epsilon_1$.

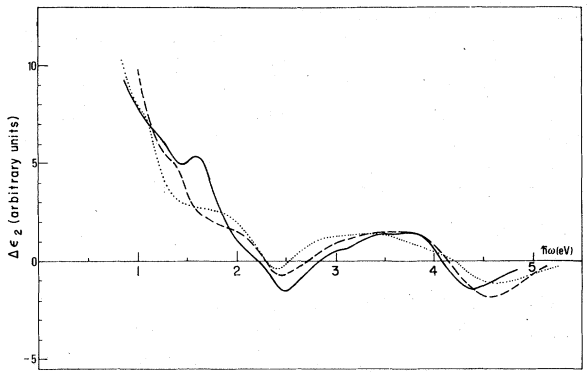

FIG. 7. Variation of the imaginary part of the dielectric function $\Delta\epsilon_2$ for Nb and Nb-Mo alloys. Full line: Nb. Dashed line: $Nb_{0.80}Mo_{0.20}$. Dotted line: $Nb_{0.50}Mo_{0.50}$.

element effects. For this reason we often are forced to make attributions without the help of recognizable line shapes.

The $\Delta\epsilon_2$ spectrum of Nb shows a peak at 1.62 eV and a shoulder at 2.26 eV, both of which are accompanied by structure in $\Delta\epsilon_1$. Upon alloying, the first structure shifts linearly to lower energies at 0.01 eV/at.%, and becomes weaker. In the 50/50 alloy this structure has shifted further toward the infrared and has become a barely perceptible shoulder. We interpret this structure as arising from $\Sigma_1(E_F) \rightarrow \Sigma_3$ transitions (near Γ). (See Fig. 5). Our CPA calculation shows that on increasing the Mo concentration in Nb, this optical gap goes to zero (when the Fermi level goes through the Γ_{25}' level), then opens up again, giving rise to $\Sigma_1 \rightarrow \Sigma_3(E_F)$ transitions.

The situation corresponding to Nb and the two alloys is shown in Fig. 5 [panels (a)–(c)]. It is interesting to note that as the Fermi level moves toward Γ, the matrix element weakens, since Σ_3 is a pure d-like level while Σ_1 is a mixture (s, p, and d) which becomes progressively more d-like on approaching Γ. This behavior is in perfect agreement with our experimental results and reinforces our attribution.

The shoulder at 2.26 eV in Nb becomes progressively more pronounced upon allying with Mo, but it does not change appreciably in energy. In $Nb_{0.50}Mo_{0.50}$ this feature has become even more distinct. The origin of this structure will become clear when discussing the molybdenum series, so we postpone its discussion.

In the high-energy region we have the contribution of an M_3 critical point at 4.5 eV. As shown in Ref. 7, this arises from transitions around the N symmetry point ($N_2 \rightarrow N_1'$). To our knowledge it is the only critical point found in the spectrum of any transition metal. Our calculations show the N_2 level to be mainly d-like while N_1' is a p-like level, making the transitions strong. Furthermore, they show the N_1' level to be very sensitive to changes in the potential. On decreasing the lattice parameter by 3% our APW calculation for pure Nb gives a change of the $N_2 \rightarrow N_1'$ gap of 0.85 eV. This large deformation potential ensures a strong signal in thermomodulation even in the presence of large lifetime broadening.

We have attempted to fit the critical point using the standard theory.[18] The results (shown in Fig. 8), assuming $E_g = 4.53$ eV and $\Gamma = 0.20$ eV, are only fair, but it should be noted that the theory is developed in the constant-matrix-element approximation. Because there is such a large width due to scattering, parts of the M_3 spectrum overlap transitions at wave vectors near that of the critical point. Since the amount of s-p-d hybridization changes rapidly away from N, the constant electric dipole matrix-element approximation is not a good one over the entire spectral structure. Moreover, it seems clear that there is another structure on the low-energy part of the $\Delta\epsilon_2$ spectrum, making perfect agreement between the measured and the calculated $\Delta R/R$ not expected.

It is interesting to note that it should be possible to see the critical point in a compositional-modulation experiment.[20] In order to simulate such an experiment we have calculated $(R^{Nb} - R^{Nb_{0.80}Mo_{0.20}})/\overline{R}$, taking the static data from Ref. 4. Since the lattice parameter shrinks upon adding Mo to Nb, we should expect the effect to have the sign reversed with respect to the thermomodulation signal. We also expect a noticeable contribution from the "modulation" of the broadening parameter, since this is liable to change significantly on alloying with 20% Mo. The "experimental" results and the attempt at a theoretical fit are shown in Fig. 9. Again the agreement is only fair. Even though we should not attach too much physical significance

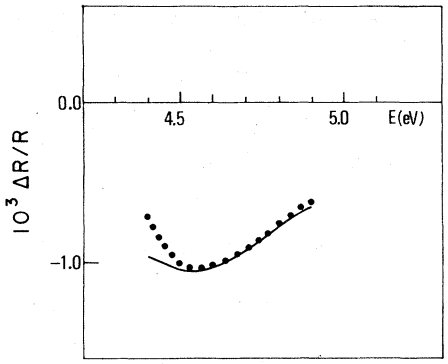

FIG. 8. Fit of the thermoreflectance spectrum of Nb in the M_3 critical point region. Dots: experiment. Full line: theory.

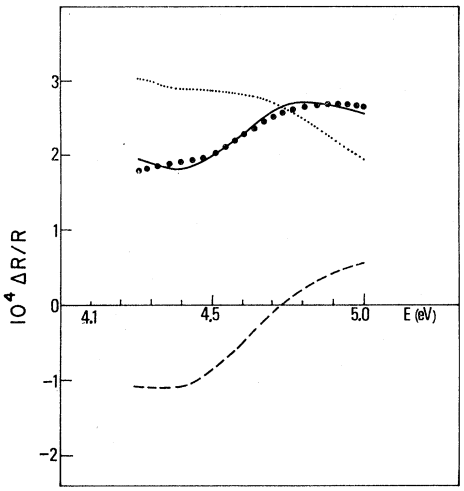

FIG. 9. Fit of the "compositional-modulation spectrum" for Nb-$Nb_{0.80}Mo_{0.20}$. Full line: theory. Full dots: "experiment." The dotted and dashed lines show the contribution of the band gap and of the broadening parameter modulation to the theoretical spectrum. The experimental data were taken from Ref. 4.

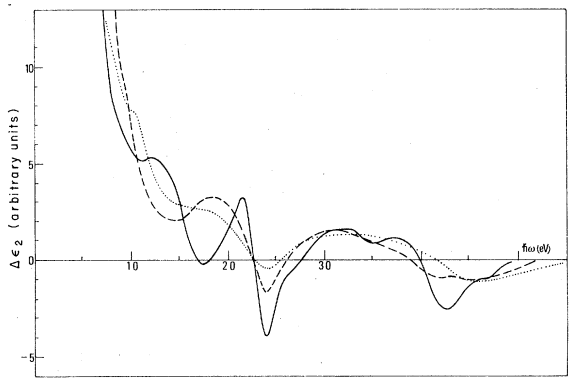

FIG. 10. Variation of the imaginary part of the dielectric function $\Delta\epsilon_2$ for Mo and Nb-Mo alloys. Full Line: Mo. Dashed line: $Nb_{0.20}Mo_{0.80}$. Dotted line: $Nb_{0.50}Mo_{0.50}$.

to the parameters used in the fit ($E_g = 4.59$ eV, $\Gamma = 0.38$ eV), the qualitative agreement corroborates our assignment.

The M_3 critical point is clearly visible also in the thermomodulation spectra of the $Nb_{0.80}M_{0.20}$ and $Nb_{0.50}Mo_{0.50}$ alloys (Fig. 7). As expected, it shifts to higher energies on adding Mo, since the lattice parameter becomes smaller.

The origin of the structure in the 3–4 eV region is not known at present, although large regions of the Brillouin zone (BZ) containing nearly parallel bands may play a role.[21]

Observing now the second series of data, starting from molybdenum (Fig. 10), we find that the first structure at 1.24 eV in $\Delta\epsilon_2$ has the appearance of a composite peak. We have a second marked feature at ~2.3 eV which has a clear derivativelike structure, indicative of a Fermi-surface transition. Upon alloying with 20% Nb this feature becomes somewhat broadened and the positive lobe has a contribution from a different transition. However, the derivativelike line shape is still clear and does not change its energy position. We are forced therefore to interpret this transition as a Fermi-surface transition between parallel bands.

A glance at the band structure reveals three possible candidates: $\Delta_5 \rightarrow \Delta_2'$, at about 1.3 eV, $\Sigma_1(E_F) \rightarrow \Sigma_3$ (near N) at ~3.2 eV, and $G_4(E_F) \rightarrow G_1$, also near N at 2.5 eV. The $\Sigma_1 \rightarrow \Sigma_3$ transitions are consistently about an eV higher in all the calculations in the literature, including ours, and may not contribute to the 2.3 eV spectrum, while the Δ transitions are too low in energy to contribute.

Going back now to the composite peak at 1.24 eV in Mo, upon alloying with 20% Nb we obtain two different structures. The first one shifts to lower energies (shoulder at 0.96 eV), while the other shifts to higher energies at 20% Nb and remains at that position for 50% Nb. Transitions $\Sigma_1 \rightarrow \Sigma_1(E_F)$ are calculated to occur at ~1.5 eV in Mo,[22] and these should shift to higher energy as Nb is added, making them candidates for one of the observed structures. Again, large regions of the BZ may be involved.[22] Transitions $\Delta_5 \rightarrow \Delta_2'$ also should contribute here. They should not shift much as Nb is added to Mo until 50% Nb is present. Then the transition energy should drop rapidly, and the transitions vanish as E_F drops below Γ_{25}' before pure Nb is reached. The role of the $\Delta_5 \rightarrow \Delta_5'$ transition is not clear at present. For this transition, a high joint density of states is expected, since the bands run parallel in a large volume of the BZ. One would expect a strong derivative signal in molybdenum at about 1.3 eV (which is indeed present in the experiment). On adding Nb, thus lowering the Fermi level, one would expect this structure to be stationary in energy, but experiment shows instead that it shifts markedly to lower energies, ruling out the $\Delta_5 \rightarrow \Delta_2'$ attribution. Our CPA calculation shows that both of these states are predominantly d-like (98–99%), so that the dipole matrix element for these transitions is presumably quite small.

At high energy the M_3 critical point is present also in molybdenum, naturally, but the line shape is more structured, indicating the presence of different contributions in the same energy region. On alloying with Nb the structure broadens and at first shifts to lower energies. (The lattice expands.) On increasing the Nb concentration the

gap jumps suddenly to higher energy (even higher than the gap for pure molybdenum), distinctly indicating a non-rigid-band behavior, as predicted by our CPA calculation in this energy region.

We believe we have carried the interpretation of the optical properties of these alloys as far as possible at present. We have also learned more about the optical properties of pure Nb and Mo, previous interpretations for Mo having been in some disagreement.[21,22] We believe that additional calculations on Nb and Mo are in order, calculations including dipole matrix elements at least in some regions of the BZ. Moreoever, a comparison of the search methods to identify structures in the joint density of states, in k space,[21] and by energy windows[22] should be made using a common set of bands. Finally, we have shown that the CPA electronic structure describes the electronic structure of Nb-Mo alloys more realistically than does the rigid-band model.

ACKNOWLEDGMENTS

This work was supported in part by the U. S. Department of Energy Contract No. W-7405-Eng-82, Division of Materials Sciences Budget Code AK-01-02-02-2, and with funds from NATO Research Grant No. 1150 (to DWL and RR). We acknowledge the technical assistance of F. Stazzi and S. Rinaldi.

[1]B. F. Schmidt and D. W. Lynch, Phys. Rev. B 3, 4015 (1971).
[2]C. J. Flaten and E. A. Stern, Phys. Rev. B 11, 638 (1975).
[3]S. Modesti, R. Rosei, and E. Colavita, Nuovo Cimento 39B, 442 (1977).
[4]E. S. Black, D. W. Lynch, and C. G. Olson, Phys. Rev. B 16, 2337 (1977).
[5]N. F. Mott and H. Jones, *The Theory of the Properties of Metals and Alloys* (Clarendon, Oxford, 1936).
[6]G. M. Stocks, B. L. Gyorffy, E. S. Giuliano, and R. Ruggeri, J. Phys. F 7, 1859 (1977).
[7]R. Rosei, E. Colavita, A. Franciosi, and J. H. Weaver (unpublished).
[8]J. H. Weaver, D. W. Lynch, C. H. Culp, and R. Rosei, Phys. Rev. B 14, 459 (1976).
[9]H. Dallaporta, J. M. Debever, and J. Hanus, Nuovo Cimento 39B, 455 (1977).
[10]J. H. Weaver, C. G. Olson, M. Piacentini, and D. W. Lynch, Solid State Commun. 16, 163 (1975).
[11]R. Rosei and D. W. Lynch, unpublished data.
[12]H. Ehrenreich and L. H. Schwartz, Solid State Phys. 31, 149 (1976).
[13]E. S. Giuliano, R. Ruggeri, B. L. Gyorffy, and G. M. Stocks, in *Transition Metals, 1977*, edited by M. J. G. Lee, J. M. Perz, and E. Fawcett (Institute of Physics, Bristol, 1978), p. 410.
[14]See, for instance, B. L. Gyorffy and G. M. Stocks, Electrons in Disordered Metals and Metallic Surfaces (edited by P. Phariseau, Plenum, to be published).
[15]B. L. Gyorffy and G. M. Stocks, in *Electrons in Finite and Infinite Structures*, edited by P. Phariseau and L. Scheire (Plenum, New York, 1977).
[16]B. L. Gyorffy, Phys. Rev. B 1, 3290 (1970).
[17]J. F. Janak, in *Computational Methods in Band Theory*, edited by P. M. Marcus, J. F. Janak, and A. R. Williams (Plenum, New York, 1971).
[18]B. Batz, in *Semiconductors and Semimetals*, edited by R. K. Willardson and A. C. Beer (Academic, New York, 1972), Vol. 9.
[19]R. Rosei and D. W. Lynch, Phys. Rev. B 5, 3883 (1972).
[20]For a description of this technique see, for instance, D. Beaglehole, Surf. Sci. 37, 708 (1973), and references therein.
[21]W. E. Pickett and P. B. Allen, Phys. Rev. B 11, 3559 (1975).
[22]See for instance J. R. Anderson, D. A. Papaconstantopoulos, J. W. McCaffrey, and J. E. Schirber, Phys. Rev. B 7, 5115 (1973) (Nb); D. D. Koelling, F. M. Mueller, and B. W. Veal, *ibid.* B 10, 1290 (1974) (Mo).